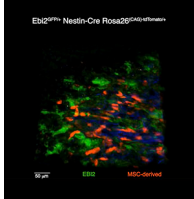
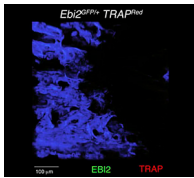


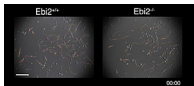
SUPPLEMENTAL MATERIAL

Nevius et al., <http://www.jem.org/cgi/content/full/jem.20150088/DC1>

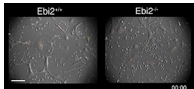
Video 1. Visualization of three-dimensional networks of EB12-expressing cells and mesenchymal stem cell (MSC)-derived cells on mouse femur BM by two-photon microscopy. Approximately 250 μm of bone tissue from *Ebi2^{GFP/+} Nestin-cre Rosa26^{(CAG)-tdTomato/+}* mice was longitudinally sectioned in a cryostat to expose bone cavity and marrow cellularity for two-photon microscopy histology. Green signal shows EB12 expression, red signal shows nestin-cre fate-mapped cells expressing Tomato fluorescent proteins, and dark blue signal shows bone matrix collagen-emitted fluorescence detected by second harmonic signal. Imaging volume is 500 \times 500 \times 100 μm (xyz, original magnification 20 \times). Data are representative of two independent mice analyzed.



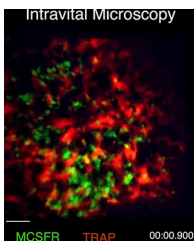
Video 2. Distribution of OCs in BM of *Ebi2^{GFP/+} TRAP^{Red}* mice by two-photon microscopy. Fixed femurs were longitudinally sectioned in a cryostat (\sim 250 μm) to expose the BM cavity for two-photon microscopy imaging. Blue indicates bone matrix collagen-emitted fluorescence detected by second harmonic signal. Imaging volume is 500 \times 500 \times 100 μm (xyz, original magnification 20 \times). Data are representative of >10 independent mice analyzed. See also Fig. 1.



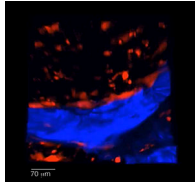
Video 3. Time-lapse microscopy of EB12-deficient and -sufficient BMDM motility in vitro. BMDMs were photographed every 2 min for 3 h (differential interference contrast, 20 \times). Cells' tracks were generated using Imaris software to generate xyz coordinates from individual cells over time. Data are representative of more than three independent experiments. This video is shown at 30 frames/s. Bar, 80 μm . See also Fig. 5.



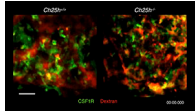
Video 4. Time-lapse microscopy of EB12-deficient and -sufficient OC motility in vitro. OCs were photographed every 3 min for 2 h (differential interference contrast, 20 \times). OC movement was examined by tracking readily distinguishable OC vacuoles over time. At least four vacuoles per OC were averaged to calculate OC velocity ($\mu\text{m}/\text{min}$) and displacement (μm). Data are representative of more than three independent experiments. This video is shown at 20 frames/s. Bar, 80 μm . See also Fig. 5.



Video 5. OCP migration and fusion with a TRAP⁺ OC in vivo. Time-lapse intravital two-photon microscopy of calvarial tissue of *CSF1R-GFP;TRAP^{Red}* double reporter mice (39- μm z stack). Monocytes and OCPs are *CSF1R⁺ (GFP⁺; green)*, and OCs are *TRAP⁺ (tdTomato⁺; red)*. The first video imaged field of view contains motile and static *CSF1R⁺* cells and largely sessile OCs. The second video shows a motile *CSF1R⁺* cell moving toward and fusing with an OC. The third video shows the same region of interest shown in the second video but rotated 180° to show cell fusion from the opposite field of view. Cell fusion is highlighted with blinking yellow arrowheads. Data are representative of three independent experiments. See also Fig. 7.



Video 6. Measurement of OC volumes by two-photon microscopy. OC differentiation in vivo from adoptively transferred FACS-sorted CSF1R⁺ precursors that overexpress tdTomato fluorescent proteins into WT recipients. Image sequence first displays bone (blue signal generated by second harmonic fluorescence) and bone-lining large tomato⁺ OCs (red). Isosurfaces were generated for red and blue fluorescence signals using Imaris. OC volumes (μm^3) were calculated from individual isosurface x, y, and z coordinates. Data are representative of three independent experiments. See also Fig. 7.



Video 7. Intravital two-photon microscopy of EBI2 signaling-deficient and -sufficient monocytes and OCPs in calvaria BM. Time-lapse intravital two-photon microscopy of calvaria BM of *Ch25h*^{+/+} (left) or *Ch25h*^{-/-} (right) M-CSFR-GFP;TRAP^{Red} double reporter mice. Blood vessels were distinguished by rhodamine-dextran (2,000 kD) injected i.v. before imaging. Data are representative of six independent experiments. This video is shown at 10 frames/s. Bar, 39 μm . See also Fig. 9.

Table S1. Dynamic histomorphometry of *Ebi2*^{+/+} and *Ebi2*^{-/-} mice

Strain	<i>n</i>	MS/BS	MAR	BFR/BS	BFR/BV	BFR/TV	SLS/BS	DLS/BS
		%	$\mu\text{m}/\text{d}$	$\mu\text{m}^3/\mu\text{m}^2/\text{yr}$	%/yr	%/yr		
WT	8	39.14 ± 11.35	1.29 ± 0.35	193.06 ± 89.69	1,161.69 ± 575.09	188.80 ± 73.51	22.63 ± 6.92	27.83 ± 9.29
<i>Ebi2</i> ^{-/-}	4	36.76 ± 7.16	1.28 ± 0.35	178.29 ± 75.34	1,073.94 ± 490.60	189.83 ± 81.83	19.74 ± 7.44	26.89 ± 7.86

Data are presented as mean ± SD. MS/BS, mineralizing surface per bone surface; MAR, mineral apposition rate; BFR/BS, bone formation rate per bone surface; BFR/BV, bone formation rate per bone volume; BFR/TV, bone formation rate per trabecular volume; SLS/BS, bone surface-referent single labeled surface; DLS/BS, bone surface-referent double labeled surface.